

# A Case Study on the LVRT Capability of an Egyptian Electrical Grid Linked to the Al-Zafarana Wind Park using Series Resistor

Ali H. Kasem \*, Heba A. Mahmoud \*\*, Adel A. Elbaset \*\*\*, Montaser Abdelsattar\*\*\*\*

\* Electrical Department, Faculty of Technology and Education, Suez University, Suez, Egypt

\*\* Electrical Department, Faculty of Technology and Education, Sohag University, Sohag, Egypt

\*\*\* Electrical Engineering Department, Faculty of Engineering, Minia University, El-Minia, and the Department of Electromechanics Engineering, Faculty of Engineering, Heliopolis University, Cairo, Egypt

\*\*\*\*Electrical Engineering Department, Faculty of Engineering, South Valley University, Qena, 83523, Egypt

(ali.alaboudy@ieec.org, Heba\_Ahmed123@techedu.sohag.edu.eg, Adel.Soliman@mu.edu.eg, Montaser.A.Elsattar@eng.svu.edu.eg)

‡Corresponding Author; Heba A. Mahmoud, Tel: +201104636796, Heba\_Ahmed123@techedu.sohag.edu.eg

*Received: 04.12.2022 Accepted: 24.01.2023*

**Abstract-** In wind farms, a doubly fed induction generator (DFIG) has proven to be the most successful wind power generator in recent years. DFIG features various speeds of operation and autonomous management of reactive and active powers. Nevertheless, the extreme DFIG sensibility to voltage dips brings a lot of defiance in terms of complying with grid code regulations set by the electrical utility operators. Now, these grid regulations impose tougher constraints, particularly for low-voltage ride-through (LVRT). Indeed, this disruption brought on by the stator circuit affects the generating system. Initially, it was necessary to turn off generators when a breakdown occurred. A disconnect could cause the entire system to fail. Recent grid codes require that in addition to meeting operating irregularities, the generators also remain connected. To increase the LVRT capacity for the Egyptian Electrical Grid linked to the Al-Zafarana Wind Park. This article introduces the design and modelling of a protection scheme employing a series resistor. The protection scheme ensures the safety of energy converters, rotor circuits, and dc-link capacitors while limiting rotor currents, dc-link voltages, and torque changes. The effectiveness of the protective scheme were also assessed for asymmetrical and symmetrical fault situations. Matlab/Simulink is used to produce the simulation findings. According to the simulation findings, the protection scheme demonstrated an effective solution for improving the LVRT feature, of the Egyptian Electrical Grid linked to the Al-Zafarana Wind Park.

**Keywords** Wind power, al-zafarana wind park, DFIG, LVRT, series resistor.

## 1. Introduction

Electric utilities struggle to supply the consumer demand for electricity because of the continuous rise in electrical energy consumption. To fulfil the rising need for energy, renewable energy sources (RESs) emerged and have advanced significantly at present [1, 2]. Since wind power is a sustainable energy source that is now promptly expanding, and has the lowest operational costs, it has taken the lead among these sources.

By 2022, the strategic objectives of the new & renewable energy authority (NREA) of Egypt, which were approved in 2008; aim to generate 20% of the total electricity from renewable energy sources, with 12% coming from wind energy systems (WES) [3, 4]. The DFIG is now most often

employed in wind farms. Given its unique characteristics like various speeds, real-reactive power management, and consistent frequency. As well as the use of lower-rated, lighter power converters with fewer losses and less mechanical pressure on the gearbox [5–8].

The DFIG turbines are more vulnerable to network outages. Due to their direct connection with the network and energy converters. Even though the fault is located far from the wind turbine (WT), it may still result in disastrous failures that impair system performance, such as blackouts and production losses. Due to this fast voltage drop, the rotor may overheat or the DC-link capacitor may overvoltage. Without protection, this causes the power converters to degrade and may even result in their destruction. Additionally, the turbine over the speed that results from them is present. The turbine

loses its ability to function normally, which causes it to be unplugged from the grid [9–11]. This aspect of DFIG led to the emergence of the LVRT capability advantage.

The capacity of a WT to maintain grid connectivity and, under specific conditions, prop it up when the grid encounters a fault, is known as LVRT capability [12, 13]. However, according to network code requirements, the WTs must be linked to the network in voltage dip situations up to a certain point and thus prop up the network. Effective LVRT schemes are crucial to propping up the grid system by controlling actual and reactive power and safeguarding energy converters in the system.

Many studies and research have addressed the issue of enhancing the ability of LVRT to DFIG in Refs. [14–19], the authors introduced the use of additional circuits. It is possible to install a crowbar circuit, a DC chopper, a series dynamic brake resistor (SDBR), a superconducting fault current limiter (SFCL), and other circuits. These methods include reducing torque fluctuations, overcurrent, and dc-link voltage. The much more typical method is to use a crowbar. This technique completely drains the grid of the reactive power required during a fault, which is very undesirable. Additionally, the rotor and controls are no longer attached, rendering the device useless. Due to the shortcomings of the crowbar circuit.

Additionally, many articles on LVRT approaches have appeared in Refs. [20–22], and LVRT approaches based on power-injecting devices are suggested. In these methods, grid voltages are regulated or optimized using devices like static synchronous series compensators (SSSC), thyristor-controlled series compensators (TCSC), static synchronous compensators (STATCOM), and dynamic voltage restorers (DVR). The ability of these devices to push or adjust active and reactive powers will consequently improve the LVRT capabilities of wind generators. Utilizing these devices increases the system's size, additionally; they are not particularly efficient in terms of cost.

Control structure-based solutions are more successful in resolving these problems. It has been mentioned in Refs. [23–26], that a combined approach of virtual resistance and demagnetizing control was employed. These structures allow for the development of a variety of system controllers to reject changes in different parameters, including electromagnetic torque, rotor current, and dc-link voltage under grid faults. Artificial intelligence (AI) techniques have also been researched because of their promise to effectively handle nonlinear challenges. Additionally, the researchers provided numerous kinds of LVRT techniques in Refs. [15, 27–29]. However, they are typically more complex and difficult to construct in practice. While extra circuits are preferred because of their simpler design process, to improve the LVRT capacity of the wind turbine powered by DFIG and linked to the Egyptian electrical grid.

This article provides a thorough analysis of the design and modelling of a protection strategy using a series resistor (SR). Controlling the rotor current is the SR's priority. By dissipating active power. It also shields the dc-link against overvoltage and torque fluctuations. As a result, the DFIG can withstand both symmetric and asymmetrical high-voltage

drops. The protection system is simulated with the MATLAB/SIMULINK tool to verify the finding.

The structure of this article is as follows: Section II describes an Al-Zafarana wind park. According to SR, Section III describes the DFIG protection scheme in full. Section IV discusses simulation modelling. The simulation findings and the impact of the SR scheme on DFIG are discussed and evaluated in Section V. Section VI presents the conclusions.

## 2. Al-Zafarana Wind Park Description

Al-Zafarana Wind Park is regarded as the biggest wind park in the Mideast. By 2022, the Al-Zafarana wind park will add 545 MW to the Egyptian electrical grid at 220 kV. This park stands out because of a variety of characteristics, including an average wind speed of 10 m/s and perfect geographic and ecological factors. Since 10 years ago, this farm has been linked to the grid in eight phases [30, 31]. Each phase is a separate wind farm project.

The projects are known as "zafarana wind farm Z1 (30 MW- 50 WT)"; "zafarana wind farm Z2 ( 33 MW- 55 WT)", "zafarana wind farm Z3 (30 MW -50 WT)", "zafarana wind farm Z4( 47 MW- 71WT)", "zafarana wind farm Z5 (85 MW-100 WT)", "zafarana wind farm Z6( 80 MW -94 WT)", "zafarana wind farm Z7( 120 MW - 141 DFIG- under install)", and "zafarana wind farm Z8( 120 MW- 141 DFIG- under install), As depicted in Fig. 1. Six wind farms have already been up and linked to the grid, and the last two phases will be finished by 2022 [32, 33]. Al-Zafarana Wind Park is a prime example of international collaboration between the Egyptian government and many nations, including Denmark, Germany, Japan, and Spain. Al-Zafarana Wind Park's designated area is 150 km<sup>2</sup>, and it is located between the latitudes of (3236) and (2906) [34, 35].

The building of many wind farms is AL-Zafarana Wind Park's key characteristic. This feature makes it easier to evaluate the effectiveness of each wind farm independently. The fifth phase of the wind farm is included for simulation purposes within this research. It comprises 100 wind turbines, each with an 850 KW DFIG unit, which makes up the system, which generates 85 MW of power in total. As shown in Fig. 2, seven feeders, served as the distribution points for the DFIGs. A 690 V/22 KV local step-up transformer serves as the connection point for each wind turbine. Three 75 MVA, 22/220 kV main step-up transformers are used to feed the gathered energy to the Egyptian electricity system at 220 kV [36].

### 2.1 WT Model

The following relationship describes the mechanical power  $P_m$  produced by the WT generators [37, 38]:

$$P_m = \frac{1}{2} C_p(\lambda, \beta) \rho A_t V_\omega^3 \quad (1)$$

Whereas the WT swept area ( $A$ ), wind speed ( $V_\omega$ ), air density ( $\rho$ ), power coefficient ( $C_p$ ), blade pitch angle ( $\beta$ ), and the turbine's angular speed to wind speed ratio ( $\lambda$ ). Following is a

definition of the relationship between the blade pitch angle and the tip speed ratio:

$$\lambda = \frac{R \omega_t}{V_\omega} \tag{3}$$

Whereas R is the radius of the WT and  $\omega_t$  is its rotating speed.

$$\begin{cases} c_p(\lambda, \beta) = 0.0068\lambda + 0.5176 \left( \frac{116}{\lambda_i} - 0.4\beta - 5 \right) \\ \frac{1}{\lambda_i} = \frac{1}{\lambda + 0.08\beta} - \frac{0.035}{\beta^3 + 1} \end{cases} \tag{2}$$

$$c_p = 0.22 \left( \frac{116}{\lambda_i} - 0.4\beta - 5 \right) e^{-12.5/\lambda_i} \tag{4}$$

With  $\frac{1}{\lambda_i} = \frac{1}{\lambda + 0.08\beta} - \frac{0.035}{\beta^2 + 1}$

The tip speed ratio is defined as follows:

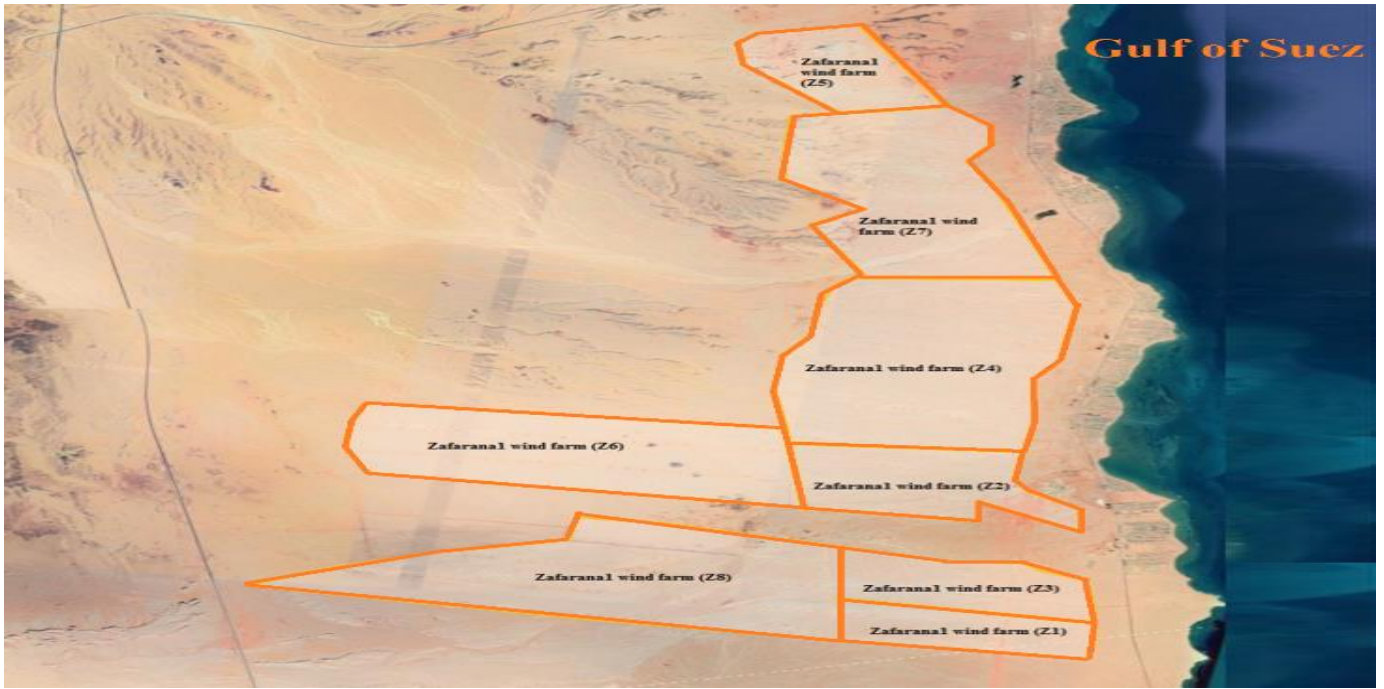
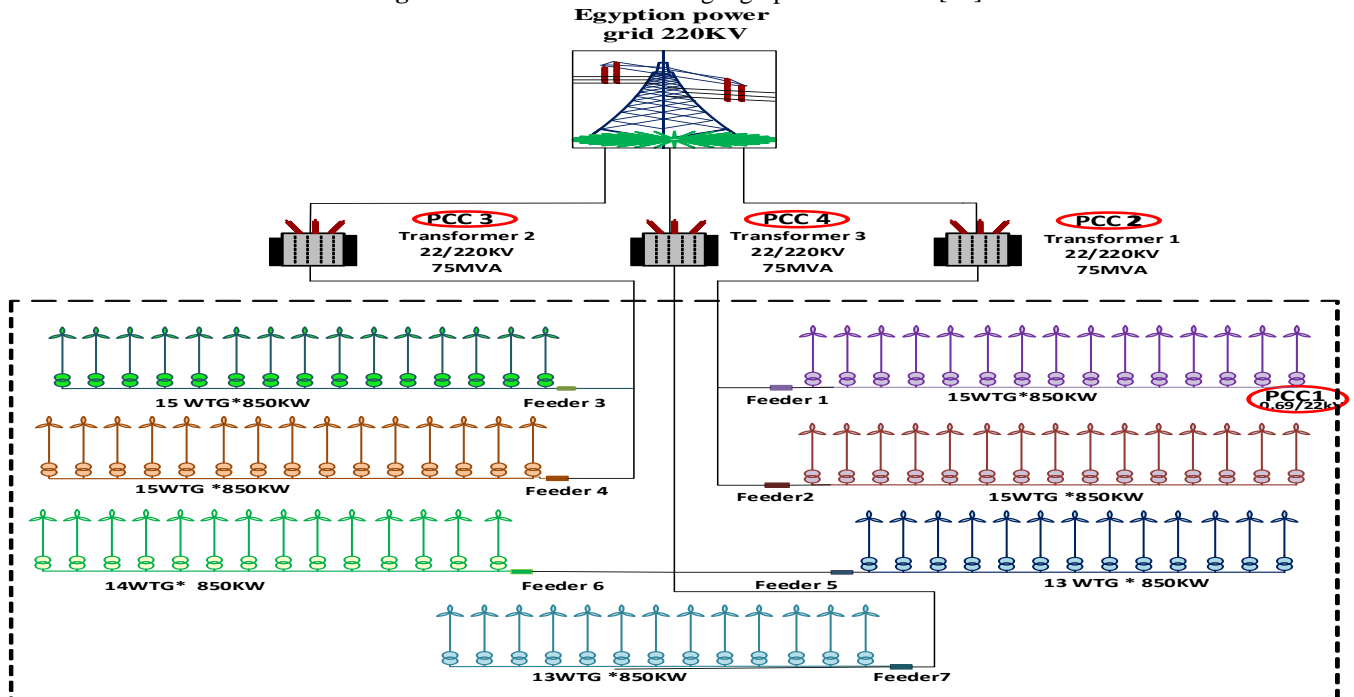


Fig. 1. Al-Zafarana wind Park geographical location [33].



Zafarana 5 (100\*Gamesa G52/850Kw)

Fig. 2. The Zafarana Z5 wind farm - simplified layout

### 2.2 DFIG Model

In modern wind energy farms, the DFIG is the most popular type of wind turbine. As illustrated in Fig. 3, the DFIG stator terminals are straight-linked to the network, and energy converters supply power to the rotor terminals. While the network side-converter keeps the dc-link voltage consistent, the rotor side-converter separately regulates the stator reactive and active energy at a steady state.

Refs. [39] provide the rotor and stator efforts in reference frames d and q.

$$\begin{cases} V_{ds} = R_s I_{ds} + P\Phi_{ds} - \omega_s \Phi_{qs} \\ V_{qs} = R_s I_{qs} + P\Phi_{qs} + \omega_s \Phi_{ds} \\ V_{dr} = R_r I_{dr} + P\Phi_{dr} - \omega_r \Phi_{qr} \\ V_{qr} = R_r I_{qr} + P\Phi_{qr} + \omega_r \Phi_{dr} \end{cases} \quad (5)$$

The fluxes of the rotor ( $\Phi_{dr}$ ,  $\Phi_{qr}$ ) and stator ( $\Phi_{ds}$ ,  $\Phi_{qs}$ ), whereas  $I_{ds}$ ,  $I_{qs}$ ,  $I_{qr}$  and  $I_{dr}$  are connected to the same q and d currents:

$$\begin{cases} \Phi_{qs} = L_s I_{qs} + M I_{qr} \\ \Phi_{ds} = L_s I_{ds} + M I_{dr} \\ \Phi_{qr} = L_r I_{qr} + M I_{qs} \\ \Phi_{dr} = L_r I_{ds} + M I_{ds} \end{cases} \quad (6)$$

Where: M is the magnetizing inductances,  $R_r$ ,  $R_s$  are the rotor and stator resistances,  $L_r$ ,  $L_s$  are the rotor and stator inductances, and  $\omega_r$ ,  $\omega_s$  are rotor speed and synchronous. The electromagnetic couple is given by:

$$T_{em} = P \frac{M}{L_s} [\Phi_{qs} I_{dr} - \Phi_{ds} I_{qr}] \quad (7)$$

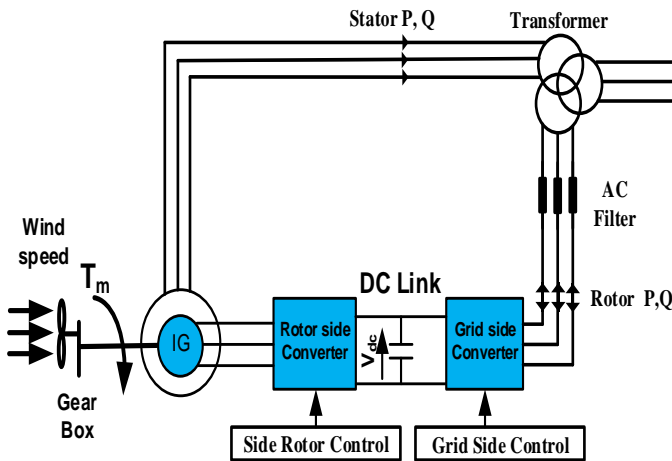


Fig. 3. The basic layout of DFIG-based WT

### 3. DFIG Protection Scheme Using Series Resistor

The SR is a group of resistors linked in series with the rotor windings in this protective scheme, as seen in Figs. 4 and 5. A power electronic switch regulates the resistance's entry into the rotor circuit. Under normal circumstances, the switch is on, bypassing the resistors. In fault situations, the switch is off, connecting the resistors in series with the rotor windings. and thus controls the over-current and over-voltage of the rotor.

It is unquestionably advantageous that the SR can control the current magnitude directly. The resistance will also split the overvoltage due to the SR's series topology. Consequently, it prevents converter control loss brought on by overvoltage and manages the robust rotor current. Limiting the current reduces the dc-link capacitor charging current, reducing the likelihood of a dc-link overvoltage.

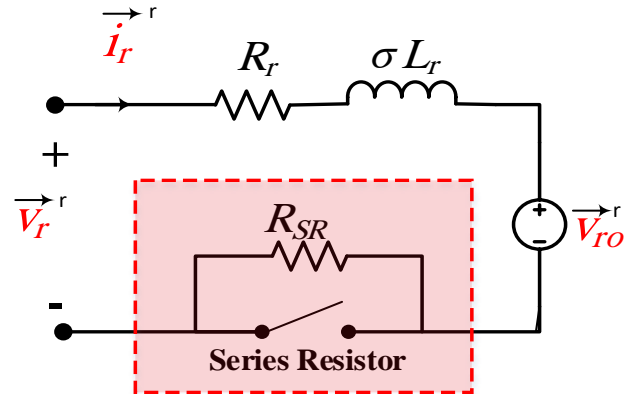


Fig. 4. Rotor equivalent circuit with a SR.

### 4. System Modelling and Simulation

The simulation paradigm of the Egyptian electricity system coupled with the WTs is shown in Fig. 6. The system being studied comprises 15 DFIG-type Gamesa (G52-850 kW), powered by 15 WTs. The WTs are coupled to a 0.96 kV/22 kV step-up transformer. The step-up transformers, 22/220 kV, 75 MVA, carry the energy from the Ain Sokhna substation to the Suez substation at 220 kV. A 220 kV gas-insulated substation switchyard connects the Suez Energy Station to the Egyptian electrical grid. The grid is represented by an equivalent voltage source incorporating internal impedance. Also, Fig. 7(a&b) displays the Simulink model of the investigated system after adding an SR protection scheme and SR Control Diagram for DFIG protection and LVRT capacity optimization. Symmetrical as well as asymmetrical faults are applied in the transmission line to investigate the LVRT capability. The entire system is modeled and the outcomes are analyzed in the MATLAB/Simulink platform. The system data is presented in Table 1.

#### 4.1 Control of Resistor SR

The control strategy is simple and easy to implement as shown in Figure 7(b), in normal operation, the switch is closed and the resistors are in bypass mode, In fault situations, the switch is open to let the current pass through the resistance.

### 5. Simulation Findings and the Impact of the SR Scheme on DFIG

This section presents the findings of using the SR scheme of DFIG protection in a variety of grid fault scenarios. When a grid failure occurs far from or near the Point of Common Coupling (PCC), the WES may be greatly impacted. The impacts might include electrical torque variations, rotor winding overcurrent, and changes in DC-link voltage. At PCC, the impacts of symmetrical and asymmetrical faults are analysed and measured. As seen in Figs. 5 and 6, the faults are simulated at the grid connection point starting at time ( $t = 0.7$  s) and ending at time ( $t = 0.9$  s), respectively.

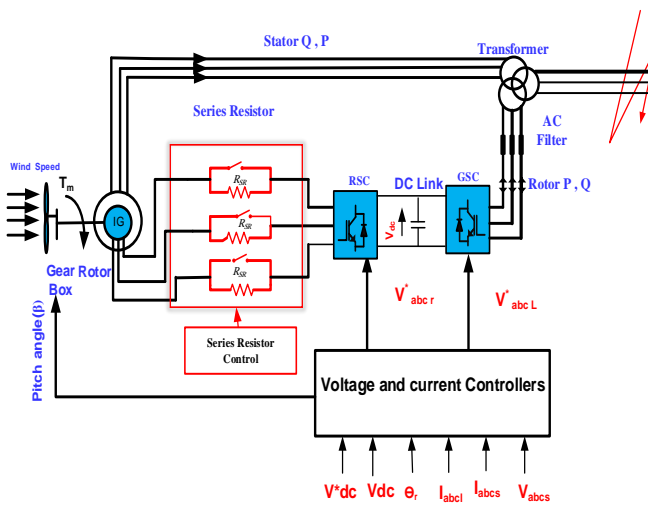


Fig. 5. DFIG configuration by series resistor

5.1 Case Study No. 1: The Symmetrical Fault

Figure 8 depicts the inception of a 3-phase fault at 0.7 s and it is clearing at 0.9 s. A 60% voltage drop occurs. It is obvious, that the SR protection scheme provides significantly faster rejection of grid disturbances. Therefore, with the addition of SR to the rotor system, the induced voltages in the rotor that surfaced during the fault lost their power. This dampens the rise in the stator and rotor currents. The stator

currents are reduced at the most severe phase from 2.1pu to 1.13pu. Additionally, during the most dangerous phase, the Rotor current decreases from 1.77pu to 1.14pu. As a result, there is a significant reduction in electrical torque fluctuations and DC link voltage. All of the values acquired from the protection technique were significantly improved, according to the study indicated above.

As displayed in Fig. 9, a 3-phase fault is simulated at the point of grid connection, commencing at the time (t = 0.7s) until clearing at the time (t = 0.9s). This diagram depicts the system's reaction to a 0.95pu effort drop lasting 0.2s. Due to the presence of SR in the rotor winding, the power from the induced efforts in the rotor that were create during the failure was dissipate in this simulation. As a result, the rise in rotor currents is reduce. As a result, the rotor currents decrease from 2.5 to 1.21 pulses per second. Additionally, the dc-link effort and electrical torque oscillations are both decreased. SR protection has a better record of accomplishment in lowering currents at the grid connection site.

5.2 Case Study No. 2: The Asymmetrical Fault

The system reactions under asymmetrical fault situations as shown in Fig. 10. The SR is efficient in dissipating the induced voltage in the rotor for a phase "a" to ground short circuit. In the most severe phase, the rotor currents also increase from 1.7pu to 1.07pu. As a result, SR greatly lowers the variations in electrical torque and the dc-link voltage. Thus, the protection plan was able to handle the serious flaw.

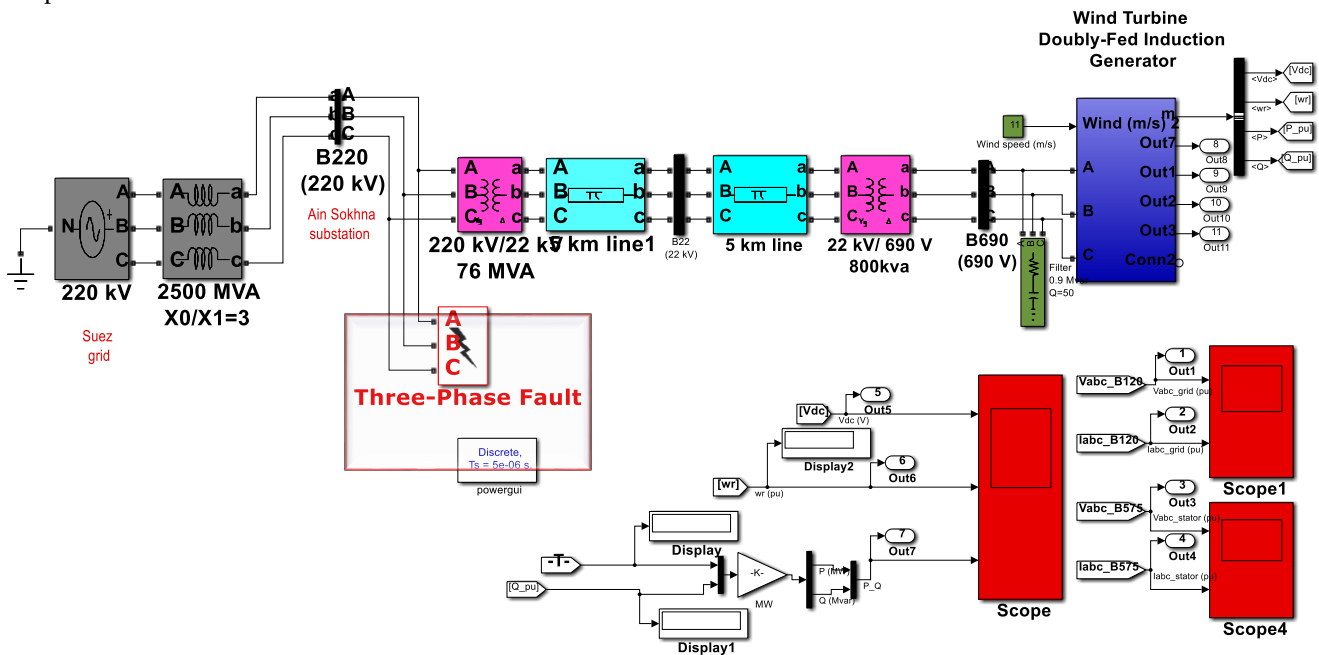


Fig. 6. Simulation paradigm of Egyptian Electrical Grid Linked to AL-Zafarana Egypt wind System.

Table1. Base and rated values for the system under investigation.

Generator		Wind Turbine	
Generator type	Asynchronous	Base wind speed (m/s)	14
Rated power(kW)	850	Cut-in wind speed	4.0 m/s
Rated voltage (V)	690	Cut-out wind speed	25.0 m/s
Number of pole pairs	2	Base rotational speed (pu)	1.2
Grid frequency (Hz )	50.0/60.0	Number of blades	3

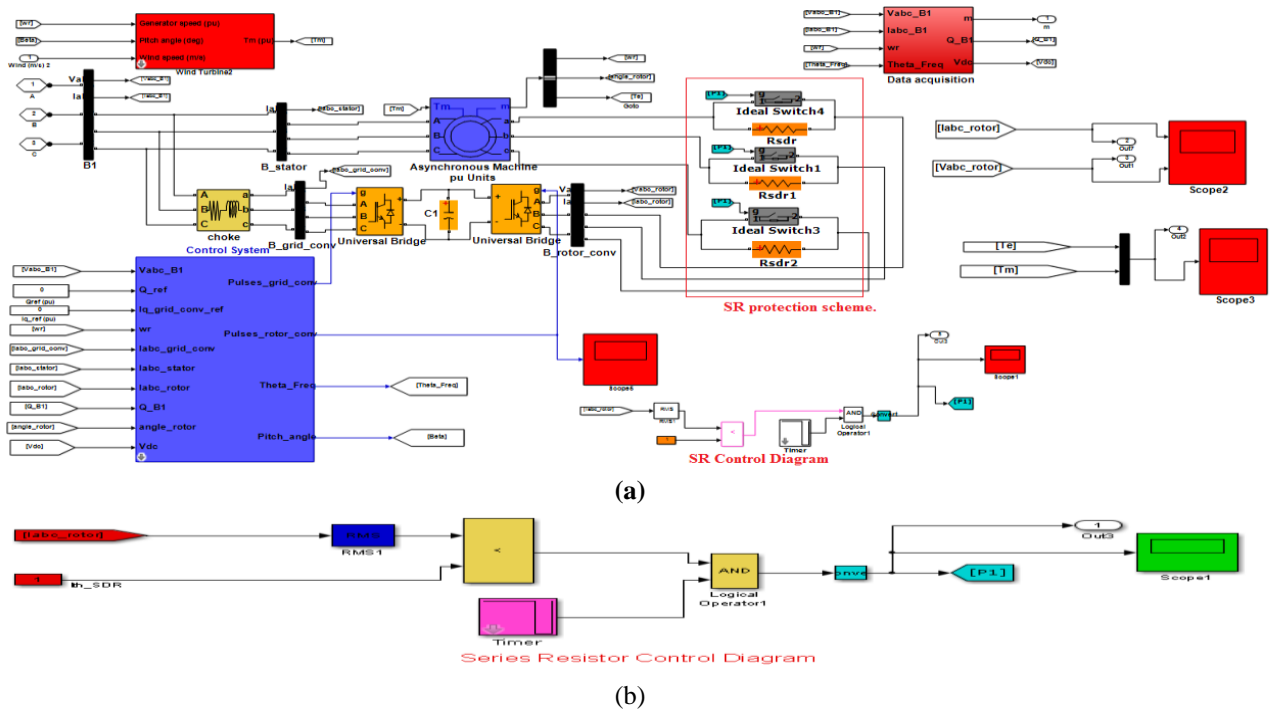


Fig. 7. A Simulink model of SR protection scheme.

A double-phase (phase-b and phase-c) fault is simulated at  $t = 0.7s$ , and Fig. 11 depicts the system reactions under asymmetrical fault circumstances. The SR is efficient in dissipating the induced voltage in the rotor when phase's "b" and "c" are short-circuited together. The rotor currents dropped from 1.91pu to 1.104pu. SR minimizes DC-link effort and electrical torque varies greatly.

Table 2 displays a comparison study between the proposed protection plan and those in the literature [40–42] based on simulation results. The proposed method provided better results in terms of damping for the currents increase at the generator terminals. Additionally, the SR scheme has built on a simple concept. It decreases the cost and complexity of the system. Hence, it contributes to system stability during grid faults.

Table 2. Comparing the results obtained from protection schemes with other works.

LVRT Techniques	Rotor Current	DC-link Voltage	Simplicity of Protection Scheme Design
Fault Current Limiter	Unacceptable	Well	Acceptable
STATCOM	Unacceptable	Acceptable	Acceptable
Energy Storage System	Unacceptable	Well	Rather complicated
Series Grid side converter	Acceptable	Well	Acceptable
Feed forward control	Acceptable	Unacceptable	Rather complicated
Series Resistor	Good	Good	Simple

## 6. Conclusion

The Egyptian electric grid with DFIG-based wind farms necessitates a turbulence reduction system to support the wind turbines' LVRT ability. The Al-Zafarana Z5 wind farm is connected to the SR protection system to enhance the system's overall performance. In this article, using an SR protection system will provide enhanced LVRT protection. The protection scheme is designed with a variety of system variables, including reactive and active energy fluctuations, rotor currents, DC link voltage, etc., that are gradually improving. Various fault scenarios have been simulated, such as:

- By applying a symmetrical 60% voltage drop, it is can be shown that SR scheme has significantly lowered the transient currents from 1.77pu to 1.14pu, Leading to the reduction of the dc-link charging current and hence lowering both the dc-link over-voltage, and torque variations. This improves the reliability of grid-connected wind energy systems. Also, by applying a symmetrical 95% voltage drop, the rotor currents is lowered from 2.5 to 1.21 pulsations per second. In addition, the electrical torque oscillations and dc-link effort is reduced. It can be demonstrated that SR protection is more successful in reducing currents at the point of grid connection.
- When a single phase is imposed on the ground, the rotor currents are reduced from 1.7pu to 1.06pu, hence improving the controllability of RSC and reducing the dc-link overvoltage. Also, under asymmetrical fault circumstances (phase-b and phase-c). The SR is efficient in dissipating the induced voltage in the rotor when phases "b" and "c" are short-circuited together. The rotor currents dropped from 1.91pu to 1.104pu. SR minimizes DC-link effort and electrical torque varies greatly.

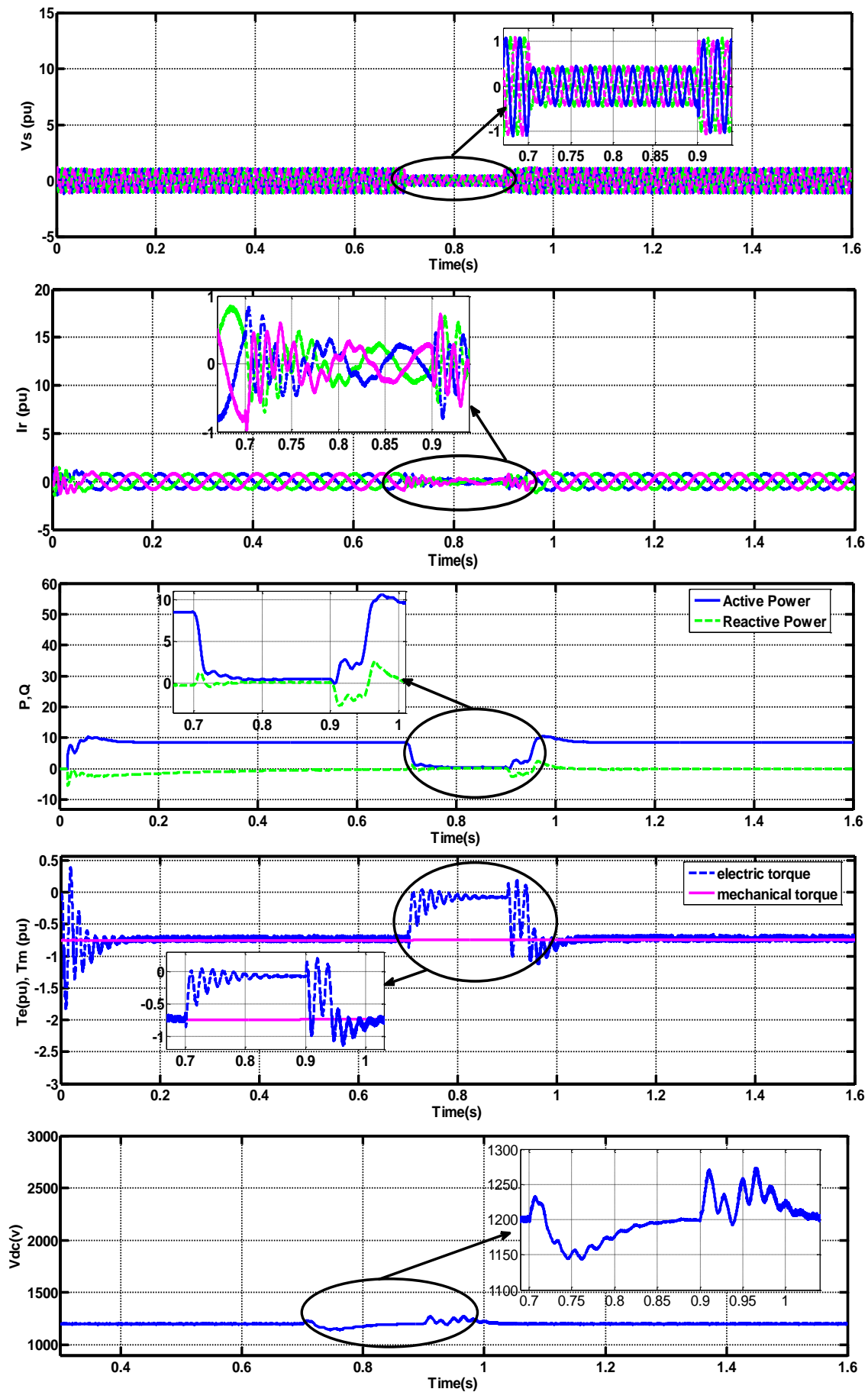


Fig. 8. The impact of the a 3-phase fault 60% effort dips on the DFIG with the SR protection scheme.

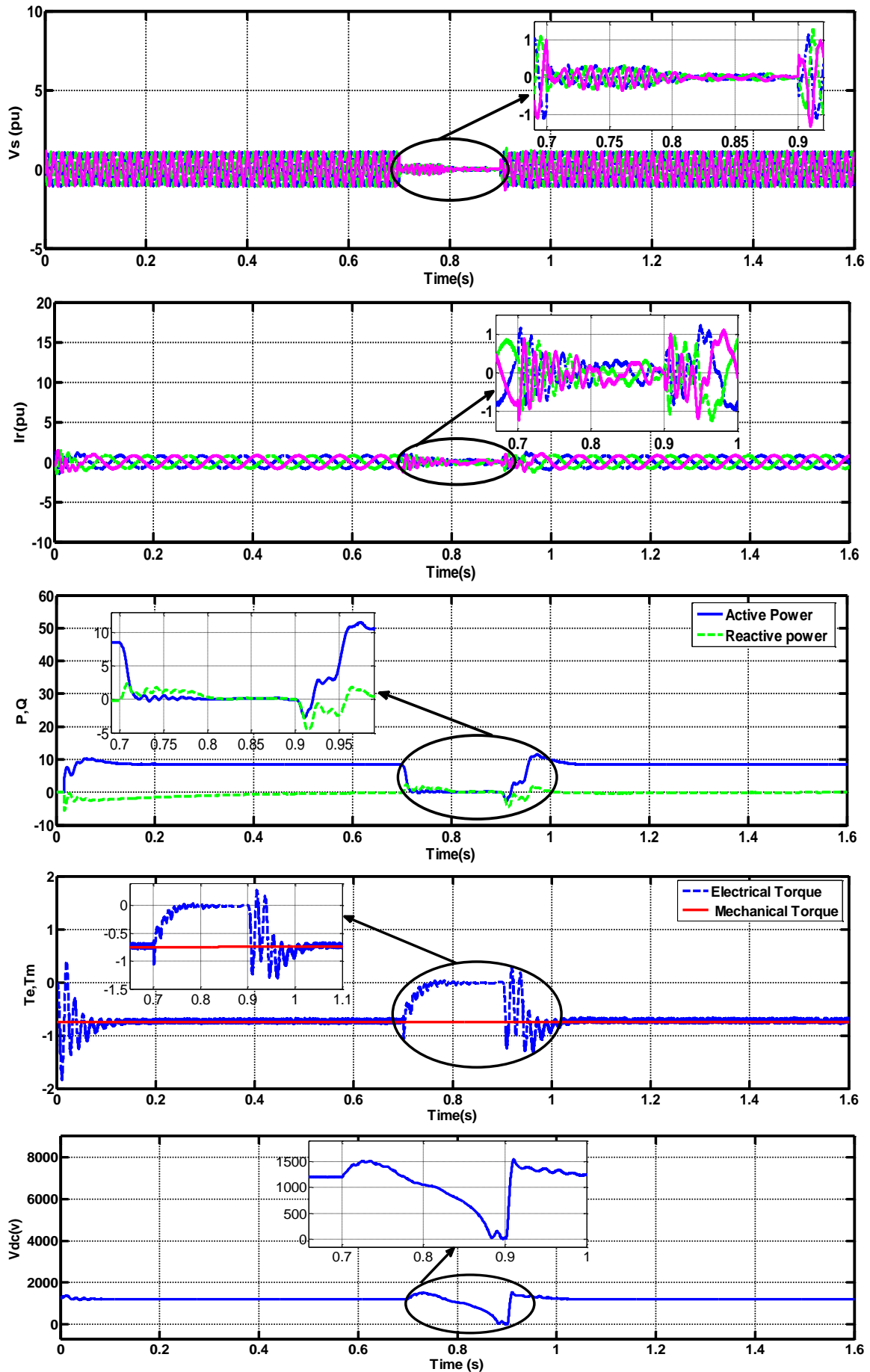


Fig. 9. The impact of a 3-phase 95% effort dips on the DFIG with the SR protection scheme.



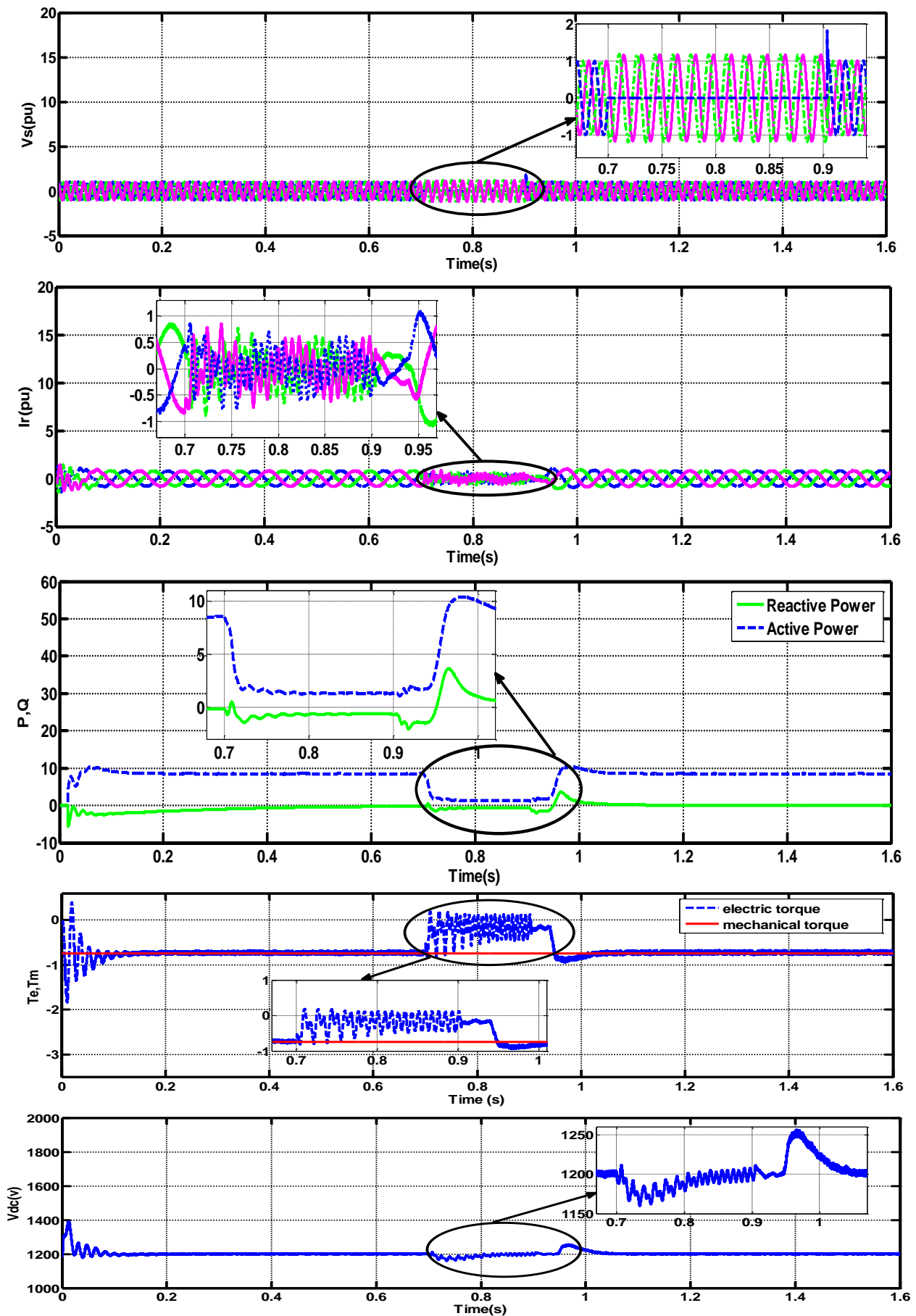


Fig. 10. The impact of the asymmetrical fault " a phase a to ground "on the DFIG with the SR protection scheme.

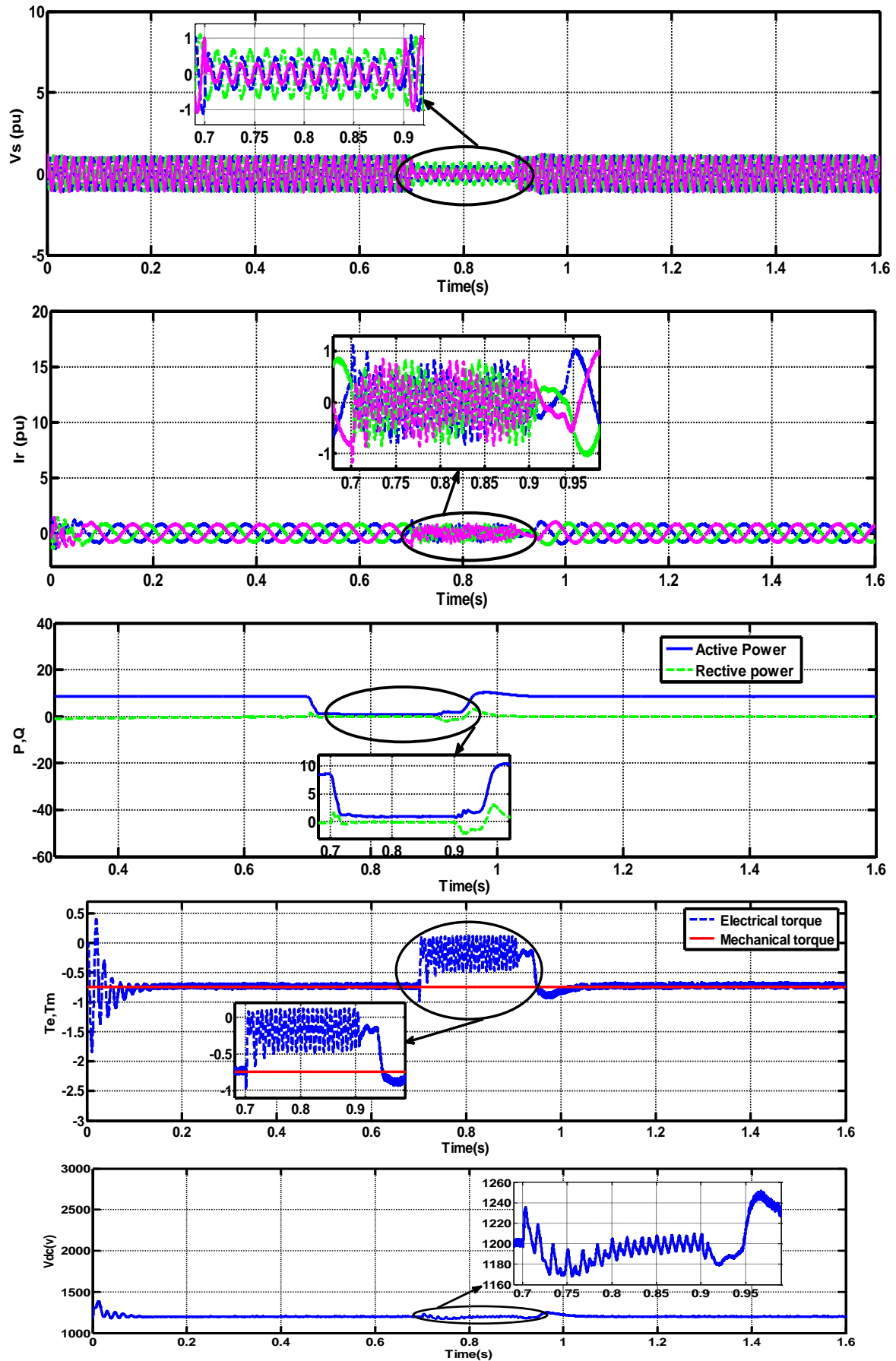


Fig. 11. The impact of the asymmetrical fault " phase b to phase c " on the DFIG with the SR protection scheme

According to simulation results, the suggested solution is characterized by handling abnormal system circumstances and supporting the grid under symmetric and asymmetric failures. The plan is also unique in that the current quantities can be directly controlled, it is simple to build, and it is inexpensive.

## References

- [1] B. Qin, H. Li, X. Zhou, J. Li, and W. Liu, "Low-Voltage Ride-Through Techniques in DFIG-Based Wind Turbines: A Review," *Applied Sciences*, vol. 10, no. 6, p. 2154, Mar. 2020, doi: 10.3390/app10062154.
- [2] E. Jamil, S. Hameed, B. Jamil, and Qurratulain, "Power quality improvement of distribution system with photovoltaic and permanent magnet synchronous generator based renewable energy farm using static synchronous compensator," *Sustainable Energy Technologies and Assessments*, vol. 35, pp. 98–116, Oct. 2019, doi: <https://doi.org/10.1016/j.seta.2019.06.006>.
- [3] O. Pfeiffer, D. Nock, and E. Baker, "Wind energy's bycatch: Offshore wind deployment impacts on hydropower operation and migratory fish," *Renewable and Sustainable Energy Reviews*, vol. 143, p. 110885, Jun. 2021, doi: <https://doi.org/10.1016/j.rser.2021.110885>.
- [4] M. Abdulrahman and D. Wood, "Wind Farm Layout Upgrade Optimization," *Energies*, vol. 12, no. 13, p. 2465, Jun. 2019, doi: 10.3390/en12132465.
- [5] S. S. Sahoo, A. Roy and K. Chatterjee, "Fault ride-through enhancement of wind energy conversion system adopting a mechanical controller," 2016 National Power Systems Conference (NPSC), Bhubaneswar, India, 2016, pp. 1-5, doi: 10.1109/NPSC.2016.7858936.
- [6] S. Bashir et al., "Development of Frequency Weighted Model Reduction Algorithm with Error Bound: Application to Doubly Fed Induction Generator Based Wind Turbines for Power System," *Electronics*, vol. 10, no. 1, p. 44, Dec. 2020, doi: 10.3390/electronics10010044.
- [7] G. Angala Parameswari and H. Habeebullah Sait, "A comprehensive review of fault ride-through capability of wind turbines with grid-connected doubly fed induction generator," *International Transactions on Electrical Energy Systems*, p. etep12395, Apr. 2020, doi: <https://doi.org/10.1002/2050-7038.12395>.
- [8] F. M. Gebru, B. Khan, and H. H. Alhelou, "Analyzing low voltage ride through capability of doubly fed induction generator based wind turbine," *Computers & Electrical Engineering*, vol. 86, p. 106727, Sep. 2020, doi: <https://doi.org/10.1016/j.compeleceng.2020.106727>.
- [9] E. El Hawatt, M. S. Hamad, K. H. Ahmed and I. F. El Arabawy, "Low voltage ride-through capability enhancement of a DFIG wind turbine using a dynamic voltage restorer with Adaptive Fuzzy PI controller," 2013 International Conference on Renewable Energy Research and Applications (ICRERA), Madrid, Spain, 2013, pp. 1234-1239, doi: 10.1109/ICRERA.2013.6749888.
- [10] F. Mazouz, S. Belkacem, G. Boukhalfa and I. Colak, "Backstepping Approach Based on Direct Power Control of a DFIG in WECS," 2021 10th International Conference on Renewable Energy Research and Application (ICRERA), Istanbul, Turkey, 2021, pp. 198-202, doi: 10.1109/ICRERA52334.2021.9598599.
- [11] O. Pfeiffer, D. Nock, and E. Baker, "Wind energy's bycatch: Offshore wind deployment impacts on hydropower operation and migratory fish," *Renewable and Sustainable Energy Reviews*, vol. 143, p. 110885, Jun. 2021, doi: <https://doi.org/10.1016/j.rser.2021.110885>.
- [12] H. Benbouhenni, H. Gasmı, and N. Bizon, "Direct Reactive and Active Power Regulation of DFIG using an Intelligent Modified Sliding-Mode Control Approach," *International Journal of Smart Grid - ijSmartGrid*, vol. 6, no. 4, pp. 157–171, Dec. 2022.
- [13] W. G. dos Santos, R. M. Monaro and M. B. C. Salles, "Discrimination on Internal and External Faults using Differential Protection Schemes for Doubly Fed Induction Generator," 2019 8th International Conference on Renewable Energy Research and Applications (ICRERA), Brasov, Romania, 2019, pp. 500-504, doi: 10.1109/ICRERA47325.2019.8997084.
- [14] Y. M. Alsmadi et al., "Detailed Investigation and Performance Improvement of the Dynamic Behavior of Grid-Connected DFIG-Based Wind Turbines Under LVRT Conditions," in *IEEE Transactions on Industry Applications*, vol. 54, no. 5, pp. 4795-4812, Sept.-Oct. 2018, doi: 10.1109/TIA.2018.2835401.
- [15] S. Tohidi and M. Behnam, "A comprehensive review of low voltage ride through of doubly fed induction wind generators," *Renewable and Sustainable Energy Reviews*, vol. 57, pp. 412–419, May 2016, doi: <https://doi.org/10.1016/j.rser.2015.12.155>.
- [16] L. Niu, X. Wang, L. Wu, F. Yan, and M. Xu, "Review of low voltage ride-through technology of doubly-fed induction generator," *The Journal of Engineering*, vol. 2019, no. 16, pp. 3106–3108, Dec. 2018, doi: <https://doi.org/10.1049/joe.2018.8443>.
- [17] K. Jayasawal and K. Thapa, "An Enhanced Low Voltage Ride-Through Control Scheme of a DFIG based WTG Using Crowbar and Braking Chopper," *Journal of the Institute of Engineering*, vol. 16, no. 1, pp. 61–67, Apr. 2021, doi: <https://doi.org/10.3126/jie.v16i1.36537>.
- [18] Z. Din, J. Zhang, Z. Xu, Y. Zhang, and J. Zhao, "Low voltage and high voltage ride-through technologies for doubly fed induction generator system: Comprehensive review and future trends," *IET Renewable Power*

- Generation, vol. 15, no. 3, pp. 614–630, Jan. 2021, doi: <https://doi.org/10.1049/rpg2.12047>.
- [19] Z. Din, J. Zhang, Y. Zhu, Z. Xu and A. El-Naggar, "Impact of Grid Impedance on LVRT Performance of DFIG System With Rotor Crowbar Technology," in *IEEE Access*, vol. 7, pp. 127999-128008, 2019, doi: 10.1109/ACCESS.2019.2938207.
- [20] A. Benali, M. Khiat, T. Allaoui and M. Denäi, "Power Quality Improvement and Low Voltage Ride Through Capability in Hybrid Wind-PV Farms Grid-Connected Using Dynamic Voltage Restorer," in *IEEE Access*, vol. 6, pp. 68634-68648, 2018, doi: 10.1109/ACCESS.2018.2878493.
- [21] G. Mokryani, P. Siano, A. Piccolo and Z. Chen, "Improving Fault Ride-Through Capability of Variable Speed Wind Turbines in Distribution Networks," in *IEEE Systems Journal*, vol. 7, no. 4, pp. 713-722, Dec. 2013, doi: 10.1109/JSYST.2012.2211812.
- [22] J. Mohammadi, S. Afsharnia, and S. Vaez-Zadeh, "Efficient fault-ride-through control strategy of DFIG-based wind turbines during the grid faults," *Energy Conversion and Management*, vol. 78, pp. 88–95, Feb. 2014, doi: <https://doi.org/10.1016/j.enconman.2013.10.029>.
- [23] S. Alaraifi, A. Moawwad, M. S. El Moursi and V. Khadkikar, "Voltage Booster Schemes for Fault Ride-Through Enhancement of Variable Speed Wind Turbines," in *IEEE Transactions on Sustainable Energy*, vol. 4, no. 4, pp. 1071-1081, Oct. 2013, doi: 10.1109/TSTE.2013.2267017.
- [24] T. D. Vrionis, X. I. Koutiva and N. A. Vovos, "A Genetic Algorithm-Based Low Voltage Ride-Through Control Strategy for Grid Connected Doubly Fed Induction Wind Generators," in *IEEE Transactions on Power Systems*, vol. 29, no. 3, pp. 1325-1334, May 2014, doi: 10.1109/TPWRS.2013.2290622.
- [25] H. Benbouhenni and H. Gasmi, "Comparative Study of Synergetic Controller with Super Twisting Algorithm for Rotor Side Inverter of DFIG," *International Journal of Smart Grid - ijSmartGrid*, vol. 6, no. 4, pp. 144–156, Dec. 2022.
- [26] A. D. Falehi and M. Rafiee, "Enhancement of DFIG-Wind Turbine's LVRT capability using novel DVR based Odd-nary Cascaded Asymmetric Multi-Level Inverter," *Eng. Sci. Technol. Int. J.*, vol. 20, no. 3, pp. 805–824, 2017.
- [27] J. M. Aga and H. T. Jadhav, "Improving fault ride-through capability of DFIG connected wind turbine system: A review," 2013 International Conference on Power, Energy and Control (ICPEC), Dindigul, India, 2013, pp. 613-618, doi: 10.1109/ICPEC.2013.6527731.
- [28] J. J. Justo, F. Mwasilu, and J.-W. Jung, "Doubly-fed induction generator based wind turbines: A comprehensive review of fault ride-through strategies," *Renewable and Sustainable Energy Reviews*, vol. 45, pp. 447–467, May 2015, doi: <https://doi.org/10.1016/j.rser.2015.01.064>.
- [29] O. P. Mahela, N. Gupta, M. Khosravy and N. Patel, "Comprehensive Overview of Low Voltage Ride Through Methods of Grid Integrated Wind Generator," in *IEEE Access*, vol. 7, pp. 99299-99326, 2019, doi: 10.1109/ACCESS.2019.2930413.
- [30] A. F. AbdelAziz, "Studying of wind farm performance at zaafarana Egypt," *International Journal of Electrical and Computer Sciences*, Vol. 11, Pp.42–51, 2011.
- [31] M. A. Ahmed, Yong Cheol Kang and Young-Chon Kim, "Modeling and simulation of ICT network architecture for cyber-physical wind energy system," 2015 IEEE International Conference on Smart Energy Grid Engineering (SEGE), Oshawa, ON, Canada, 2015, pp. 1-6, doi: 10.1109/SEGE.2015.7324601.
- [32] M. M. A. Mahfouz, A. M. Amin and E. B. Youssef, "Improvement the Integration of Zafarana Wind Farm Connected to Egyptian Unified Power Grid," 2011 46th International Universities' Power Engineering Conference (UPEC), Soest, Germany, 2011, pp. 1-6.
- [33] A. Fouad, M. Elshahed, M. Sayed, and M. Gilany, "Harmonic resonance overvoltage due to main transformer energization in large wind farms, Zafarana, Egypt," *Ain Shams Engineering Journal*, vol. 10, no. 4, pp. 731–743, Dec. 2019, doi: <https://doi.org/10.1016/j.asej.2019.04.002>.
- [34] New and renewable energy authority in Egypt (NREA), Annual report. Egypt, NREA; 2019. Available: <http://nrea.gov.eg/Content/reports/English%20AnnualReport%20percentage202019.pdf>, [Accessed 29 November 2022].
- [35] New and renewable energy authority in Egypt (NREA), Annual report. Egypt: NREA; 2015. Available: [http://www.moee.gov.eg/english\\_new/eehc\\_rep/2015-2016en.pdf](http://www.moee.gov.eg/english_new/eehc_rep/2015-2016en.pdf), [Accessed 29 November 2022].
- [36] M. G. Hemeida, H. Rezk, and M. M. Hamada, "A comprehensive comparison of STATCOM versus SVC-based fuzzy controller for stability improvement of wind farm connected to multi-machine power system," *Electrical Engineering*, vol. 100, no. 2, pp. 935–951, May 2017, doi: <https://doi.org/10.1007/s00202-017-0559-6>.
- [37] M. Venkatesh, T. S. L. V. Ayyarao, B. S. Rao, R. Raghu and R. S. S. Nuvvula, "A Robust Wide Area Control of DFIG Wind Energy System for Damping Inter-area Oscillations," 2022 11th International Conference on Renewable Energy Research and

- Application (ICRERA), Istanbul, Turkey, 2022, pp. 28-32, doi: 10.1109/ICRERA55966.2022.9922717.
- [38] A. A. Chhipa et al., "Modeling and Control Strategy of Wind Energy Conversion System with Grid-Connected Doubly-Fed Induction Generator," *Energies*, vol. 15, no. 18, p. 6694, Sep. 2022, doi: 10.3390/en15186694.
- [39] M. Kendzi and A. Aissaoui, "Comparison Between the MIT Rule and Fuzzy Logic Controller to Adapting the Power Generated by a Doubly Fed Induction Generator Integrated in a Wind System," 2022 10th International Conference on Smart Grid (icSmartGrid), Istanbul, Turkey, 2022, pp. 231-235, doi: 10.1109/icSmartGrid55722.2022.9848520..
- [40] L. Saihi, Y. Bakou, A. Harrouz, M. Boura, I. Colak and K. Kayisli, "Robust Sensor-less SMC under Variable-Speed Wind Turbine Systems of DFIG based on FKE," 2022 10th International Conference on Smart Grid (icSmartGrid), Istanbul, Turkey, 2022, pp. 301-305, doi: 10.1109/icSmartGrid55722.2022.9848578.
- [41] A. Rini Ann Jerin, P. Kaliannan, U. Subramaniam, and M. Shawky El Moursi, "Review on FRT solutions for improving transient stability in DFIG-WTs," *IET Renewable Power Generation*, vol. 12, no. 15, pp. 1786–1799, Oct. 2018, doi: <https://doi.org/10.1049/iet-rpg.2018.5249>.
- [42] M. Amer Saeed, H. Mehroz Khan, A. Ashraf, and S. Aftab Qureshi, "Analyzing effectiveness of LVRT techniques for DFIG wind turbine system and implementation of hybrid combination with control schemes," *Renewable and Sustainable Energy Reviews*, vol. 81, pp. 2487–2501, Jan. 2018, doi: <https://doi.org/10.1016/j.rser.2017.06.054>.